Proc. Natl. Acad. Sci. USA
Vol. 73, No. 11, pp. 4027–4031, November 1976
Cell Biology

Collagen fibrillogenesis: Intermediate aggregates and suprafibrillar order

(morphogenesis/self assembly/polymerization)

ROBERT L. TRELSTAD, KIMIKO HAYASHI, AND JEROME GROSS

The Developmental Biology Laboratory, Departments of Medicine and Pathology, Massachusetts General Hospital, and Harvard Medical School, Boston, Mass. 02114

Contributed by Jerome Gross, July 19, 1976

ABSTRACT **Polymerization of collagen *in vitro* has been studied with the electron microscope at early time points of fibril assembly. We have found morphologically distinct stages of aggregation, which we suggest represent successive steps in fibril formation. Linear growth of the fibril appears to occur by the tandem addition of aggregates to each other and subsequently to the ends of a subfibril; lateral growth occurs by the entwining, like a rope, of these subfibrils. Fibrillogenesis is also accompanied by extensive development of suprafibrillar order in which various patterns of parallel, spiral, and orthogonal sets of fibrils were frequently observed.**

The form in which newly synthesized collagen molecules are excreted into the extracellular space and organized into striated fibrils in ordered tissue patterns has long intrigued those interested in morphogenesis. We now know that collagen is synthesized in a precursor form which requires the excision of both carboxy- and amino-terminal peptides prior to normal fibril formation (1–3). Because the denaturation temperature of dispersed native collagen molecules (t_m = 32–40°) is in the physiologic temperature range, the potential existence of newly synthesized collagen in molecular dispersion in the tissue prior to organization into fibrils remains a puzzle. Studies on fibril formation *in vitro* indicate that upon aggregation into fibrils, but prior to intermolecular crosslinking, the thermal stability of the collagen increases (4). In addition, there are strong indications that newly synthesized collagen (or procollagen) is packaged in the cytoplasm in membrane-bound vacuoles containing molecular aggregates that are then excreted into the extracellular space (5–7). Such aggregates would have the required thermal stability to resist denaturation at body temperature.

We are proposing the possibility that such aggregates are true intermediates of fibril formation as an alternative to the idea of a cloud of dispersed procollagen molecules which accrete individually onto a growing fibril. Ordering within the subsequent fibrous array of intermediate aggregates would then occur consequent to the enzymatic removal of terminal peptides.

MATERIALS AND METHODS

A number of different sources of collagens were used: fetal calf skin, rat tail tendon, lathyritic chick tendon and skin, wallaby tail tendon, and guinea pig skin. Extracts of neutral-salt-soluble collagen were prepared using 0.4 ionic strength (Γ/2) potassium phosphate buffer, pH 7.6, and were purified by repeated NaCl precipitation at both neutral and acidic pH. The purified collagen was desalted by dialysis after resolubilization in 0.1 M acetic acid and stored as an acidic solution, or as the salt precipitate (7% NaCl) of an acidic solution or after lyophilization.

Purity determination and characterization of the collagen were by amino acid analysis, CM-cellulose chromatography, and molecular sieve chromatography as previously described (8).

Fresh solutions of the purified collagens were prepared at 4° from the stored materials in either 0.2 Γ/2 phosphate buffer, pH 7.6, or 0.15 M NaCl in 0.02 Γ/2 phosphate buffer, pH 7.6. The lyophilized collagens were stirred directly into the buffers, whereas the salt precipitate or acid solutions were dialyzed against the neutral buffer. The solutions at concentrations varying from 0.001 to 1.0 mg/ml were clarified by centrifugation at 100,000 × *g* for 2 hr at 4° prior to use.

Gelation of the neutral collagen solutions was accomplished in a 37° humidified incubator. The solutions were either placed directly onto collodion-coated copper grids or as a drop in a plastic petri dish. With the latter method the sample was applied to the grid by immersing it into the semi-gelled solution, by pipetting onto the grid or by touching the grid to the drop.

The excess solution was drained carefully by touching the edge of the grid to filter paper and the specimen was rinsed with distilled water, air dried, and stained. Negative staining was done using a 1% solution of phosphotungstic acid, pH 9.0, for 5–10 min. For positive staining the grids were exposed to 0.1% ATP in 0.4 Γ/2 phosphate buffer, pH 7.6, for 10 min, rinsed, and then stained with saturated aqueous uranyl acetate for 15–30 min. The grids were examined in an RCA EMU 3G or JEM 100 B electron microscope.

Photographic enhancement of the positively stained preparation of aggregates was achieved using narrowly masked negatives and a linear translational device for even lateral movement of the photographic paper (9).

RESULTS

The ultrastructural data described below were similar for the five different sources of collagen, although the bulk of the study was conducted with that from the lathyritic chick skin. Biochemical analyses of the purified collagens indicated the preparations studied contained only Type I collagen; noncollagen proteins were not detectable.

The Initial Aggregate: Negatively Stained. Freshly prepared neutral solutions of lathyritic collagen, prepared from nonlyophilized purified stocks, appeared predominantly as a cloud of nonstructural material. (Fig. 1). Similar observations were made on solutions prepared from the lyophilized lathyritic chick collagens, or from any of the nonlathyritic preparations, but in addition these showed a number of early aggregates, similar to those to be described below, despite vigorous centrifugation (10). If nonlyophilized lathyritic stocks were stored in neutral condition at 4° for more than 1–2 days, aggregates were apparent.

The first aggregates formed upon heating for 15 min or less

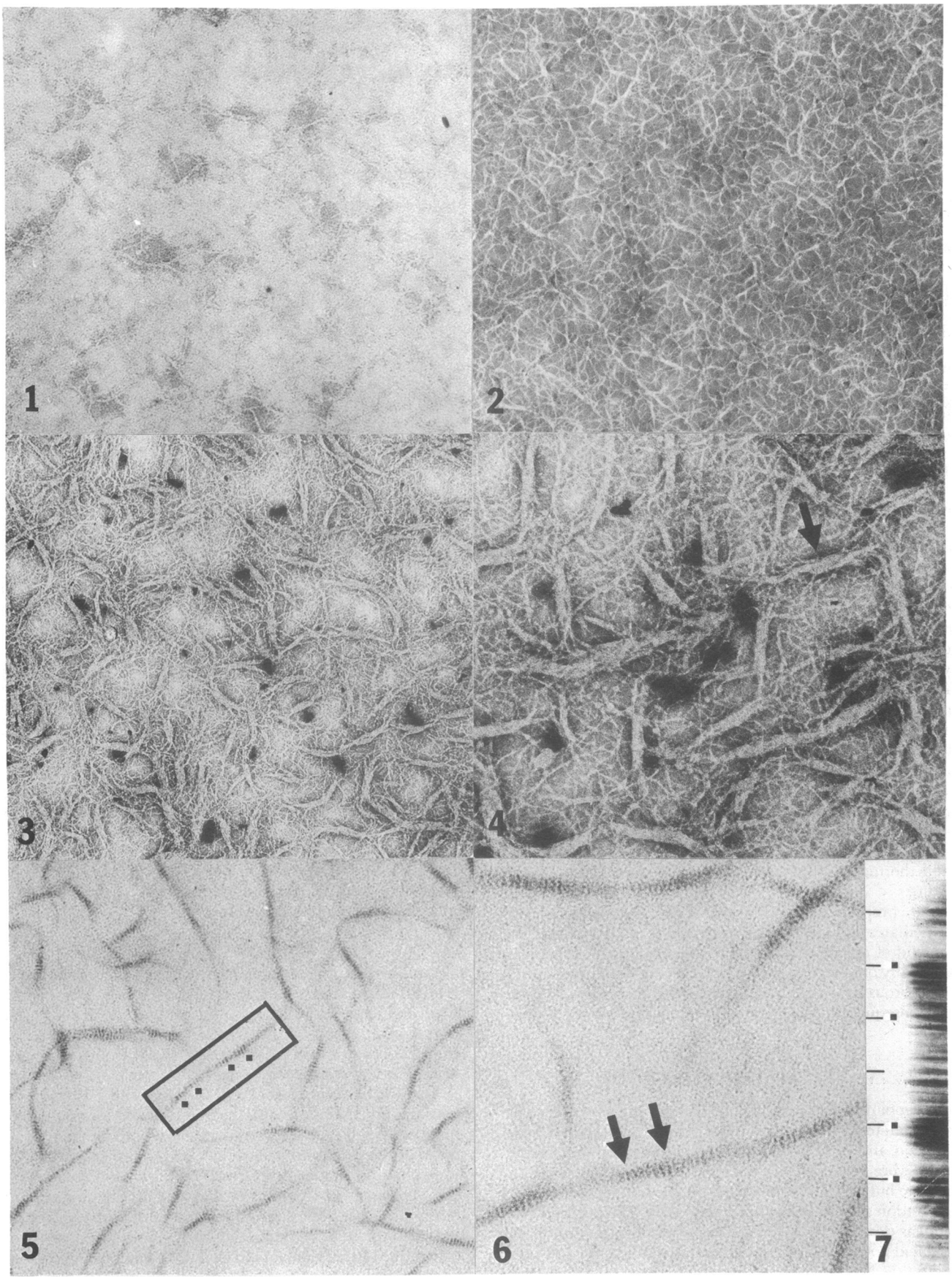

FIGS. 1–7. (*Legend appears at bottom of the following page.*)

varied in diameter, depending on the initial collagen concentration (Table 1). The lowest concentration at which aggregates could be reliably observed was 0.001 mg/ml, at which they were quite narrow, with a diameter of approximately 5 nm (Fig. 2). Aggregates with similar diameters were seen up to concentrations of about 0.01 mg/ml, above which wider structures were observed (Table 1). Those that had a diameter of 5 nm appeared to represent a discrete structure somewhat independent of concentration in that they were the predominant form observed over a 10-fold range of collagen concentration (0.001–0.01 mg/ml). Moreover, similar narrow, 5 nm wide aggregates were also seen at higher concentrations, but usually in lateral association with other similarly sized structures (Figs. 3 and 4). The 5 nm wide aggregate is hereafter referred to as a *limiting initial aggregate*, whereas the structures resembling laterally associated groups of limiting initial aggregates are called *initial aggregates*. The typical aggregates formed at 0.5–1.0 mg/ml (Figs. 3, 4, 8–10) appeared to consist of laterally associated limiting initial aggregates, often in an entwined configuration with a more compact central portion and frayed ends.

The length of the limiting initial aggregate as well as that of the wider initial aggregates was difficult to evaluate accurately. The ends of the structures were not clearly resolved and efforts to disperse the aggregates to better separate their apparently overlapping ends were unsuccessful. The length of the more compactly entwined central portion of the initial aggregate was about 300 nm. If the measurement included the splayed narrow ends, lengths of 1000 nm were common.

The Initial Aggregates: Positively Stained. Efforts to stain positively the initial aggregates with both acidic phosphotungstic acid and/or uranyl acetate at various concentrations, pH values, and buffers were only intermittently successful. However, reproducible staining was achieved by "prestaining" the air-dried aggregate on the grid with a 0.1% neutral solution of ATP.

Positively stained initial aggregates revealed structures with a distinct cross-striated appearance. The stained structures were tapered, and resembled the initial aggregates seen in negative contrast. The pattern of cross striations suggests that a form of staggered packing resembling that of the mature fibril is present, since a macroperiod of 67 nm can be seen (Figs. 5–7).

The Early Linear Fibrillar Aggregate. After 15 min at 37° linear fibrillar structures of fairly uniform diameter appeared, which were similar in width to the initial aggregates present in the same field (Figs. 8–10). The linear fibrillar aggregates or subfibrils often lay in near parallel register (Fig. 8). These linear aggregates were often branched and adjacent subfibrils in the lateral parallel array may thus be linked together. In many cases unstriated and striated fibrils constituted one continuous structure (Figs. 9 and 10).

Initial aggregates were frequently seen near the ends of linear fibrillar aggregates and the frequency of such associations suggests that linear fibrillar aggregates form by the tandem association of initial aggregates and that the growth of the linear aggregate occurs by successive addition to the ends of the fibril (Figs. 8–11).

Table 1. Concentration dependence of initial aggregate width

Collagen concentration (mg/ml)	Initial aggregate width (nm)*
1.0	25
0.5	18
0.1	15
0.05	10
0.01	5
0.005	5
0.001	5

* Values for width were obtained from micrographs after calibration of the microscope with a carbon grating replica (2160 lines per mm). The measurements of more than 100 aggregates for each concentration fell within a range of ±10% of the noted value. After averaging the value was rounded to the nearest integer.

The Striated Fibril. Structures with the typical appearance of native cross-striated fibrils began to appear between 30 and 60 min following incubation. These striated fibrils were often seen within fields of linear unstriated fibrils; frequently both forms were continuous. The striated fibrils often were entwined to form loose rope-like structures (Fig. 11). The growth in width of the fibril thus appears to involve the lateral association of the linear unstriated fibrils, apparently twisted as a group about the long axis of the forming fibril.

Inhibition of Fibrillogenesis. Since Tris·HCl, glucose, and arginine have previously been shown to interfere with collagen fibrillogenesis (11, 12), we examined the effects of various concentrations of these substances on fibril formation. Collagen aggregation into initial aggregates was not prevented, but at concentrations above 0.1 M for each substance formation of fibrillar forms was precluded. A systematic and quantitative evaluation of these and other compounds has not been done, but the effects are readily reversible after removal of the inhibitors by dialysis.

Pattern Formation. A striking feature of the heat gels was the formation of ordered suprafibrillar patterns of aggregation (Figs. 8, 12, and 13). This was most prominent in preparations examined between 15 and 30 min of gelation, when the principal structures present were the early linear fibrils. Often ordered arrays of fibrils were clearly separated by less ordered regions (Fig. 8). The most common pattern was simple linear alignment (Fig. 8). However, other patterns were also observed, including orthogonal (Fig. 12) and spiral (Fig. 13) configurations.

FIGS. 1–7 (*on preceding page*). All figures are electron micrographs of lathyritic collagen aggregates. The collagen concentration of the solutions was 0.5 mg/ml except for that shown in Figs. 3 and 4, in which it was 1.0 mg/ml. *Fig. 1.* Zero time control at 4°. Phosphotungstic acid, pH 9.0. ×72,750. *Fig. 2.* Limiting initial aggregates, formed after heating at 37° for 5 min. Phosphotungstic acid, pH 9.0. ×58,200. *Fig. 3.* Fusiform initial aggregates with an average diameter of 27 nm after 15 minutes at 37°. The ends of the aggregates are splayed and the initial aggregate clearly is formed from laterally associated narrower structures. Phosphotungstic acid, pH 9.0. ×40,160. *Fig. 4.* Higher magnification of the initial aggregates, illustrating their twisted configuration (arrow), splayed ends, and derivation from narrower materials. Phosphotungstic acid, pH 9.0. ×79,100. *Fig. 5.* Initial aggregates stained positively with uranyl acetate. Cross striations are present with a macroperiod of 67 nm. The rectangle encloses two aggregates in tandem alignment, each with 67 nm striations as indicated by the closed squares. A region such as outlined in the rectangle was used for photographic enhancement (Fig. 7). Uranyl acetate, pH 3.4. ×50,450. *Fig. 6.* Higher magnification of the positively stained initial aggregates, showing the macroperiod of 67 nm (arrows). Uranyl acetate, pH 3.4. ×121,100. *Fig. 7.* A region such as outlined in the rectangle on Fig. 5 was projected onto photographic paper which was laterally translated during exposure. The drawn lines on the left are spaced at 67 nm. The striations indicated by the closed squares correspond to those within the rectangle in Fig. 5. ×144,550.

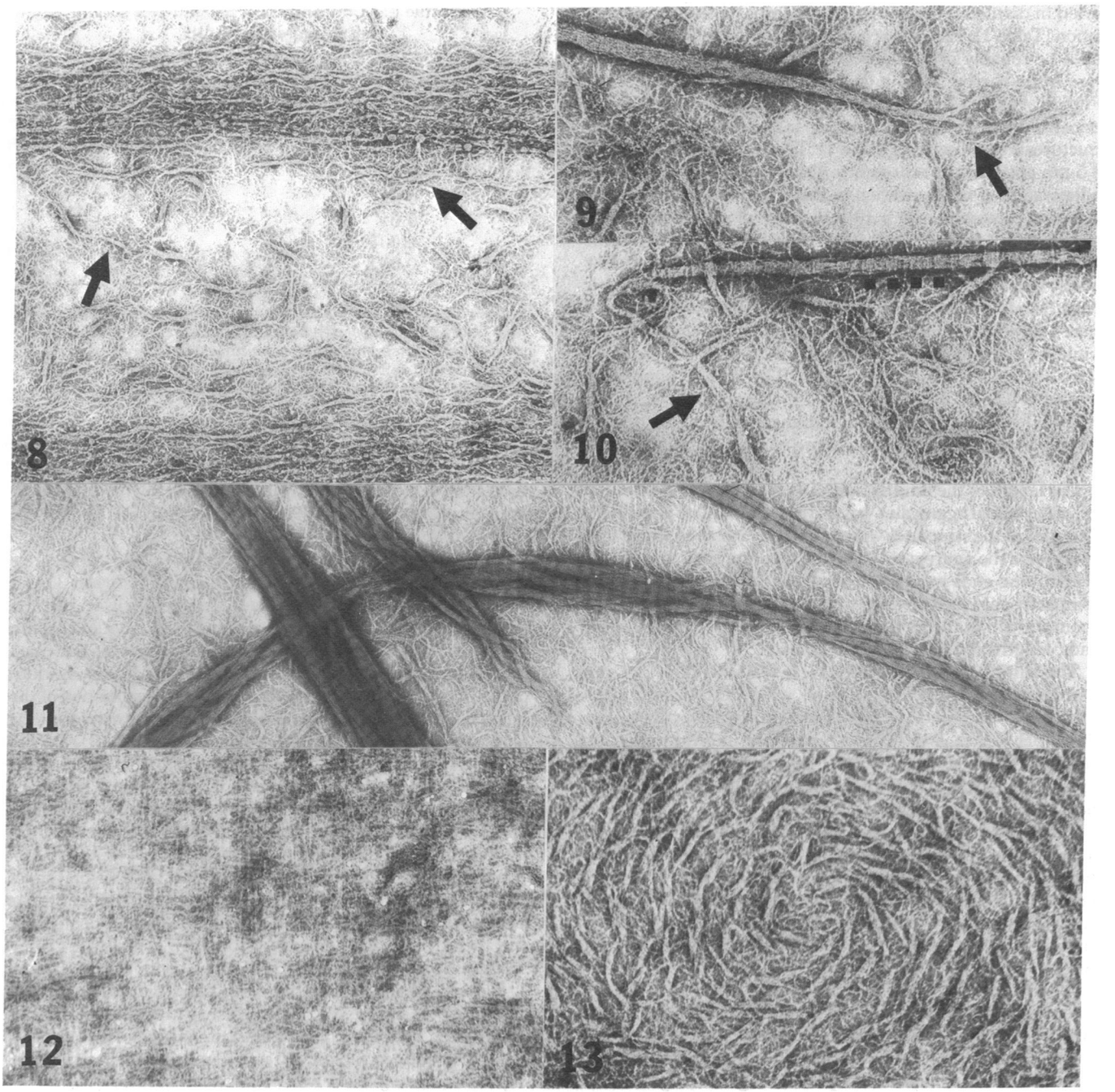

FIGS. 8–13. All figures are electron micrographs of lathyritic collagen aggregates. The collagen concentration of the solutions was 0.5 mg/ml except for that shown in Fig. 12, in which it was 0.05 mg/ml. *Fig. 8.* Initial aggregates and linear fibrillar aggregates after 15–30 min gelation. Two separate sets of fibrillar aggregates are forming with similar orientation. A number of examples of tandemly arranged initial aggregates are apparent (arrows). Phosphotungstic acid, pH 9.0. ×60,000. *Figs. 9 and 10.* Solutions heated 15–30 min at 37°, showing the ends of linear fibrillar aggregates in close association with initial aggregates. In both figures examples of tandemly arrayed initial aggregates are seen (arrows). A macroperiod of 67 nm is beginning to become apparent in the negatively stained fibrillar aggregates (closed squares). Phosphotungstic acid, pH 9.0. ×60,000. *Fig. 11.* A neutral solution previously inhibited from forming fibrils by Tris·HCl was dialyzed against phosphate buffer at 37° to remove the inhibitor and was sampled after 15 min. Fibril formation in such preparations is unusually rapid and all stages from the limiting initial aggregates to fully formed fibril are present. The fibrils show obvious 67 nm cross striations, tapered ends in association with initial aggregates, and a rope-like twisting together of the linear fibrillar forms. Phosphotungstic acid, pH 9.0. ×34,000. *Figs. 12 and 13.* Suprafibrillar patterns are common in solutions stored at 4° prior to study. The geometric patterns are several, including parallel (Fig. 8), orthogonal (Fig. 12), and spiral (Fig. 13). Phosphotungstic acid, pH 9.0. Fig. 12 ×52,000; Fig. 13 ×52,500.

Pattern formation could be enhanced by preincubation of the neutral solution on the grid or in the petri dish at 4° for 1 or more days.

DISCUSSION

The initial model for collagen fibrillogenesis *in vivo* was based on the observations that purified solutions of collagen under physiological conditions *in vitro* assemble spontaneously into typical cross-striated fibrils (13). A long-prevailing idea held that collagen was excreted by the cell as a monomer and diffused away into the matrix where it precipitated with other monomers to form a fibril.

The observations reported here suggest that the polymerization of collagen is not a simple one-step, monomer–polymer transition, but rather occurs in several distinct stages involving subassemblies. We propose that the subassemblies described here are morphogenetic intermediates involved in step-wise association to fibrils and reflect the situation in fibrillogenesis *in vivo* perhaps during and after enzymatic processing of packets of procollagen molecules.

Physical chemical studies of collagen polymerization *in vitro* have demonstrated lag and growth phases and suggest that structures formed during lag phase serve as nuclei for subsequent collagen polymerization (12, 14). The physical and ultrastructural properties of these "nuclei," however, have not been described, but they coincide temporally in the gelation process with the initial aggregates.

Recent refinements of the three-dimensional structure of the collagen fibril suggest that a basic structural element of the fibril is a microfibril with a 4 nm diameter and 67 nm axial periodicity consisting of five quarter-staggered collagen molecules (15). Our observations indicate that, at very low concentrations, limiting initial aggregates approximately 5 nm in diameter are always present and could represent the microfibril. We would suggest, however, that initially these aggregates are limited in length, and often in a loosely entwined lateral relationship with one another to form the next subassembly, the initial aggregate. Its intermolecular order, i.e., the 1D or near quarter stagger, would be reflected in the repeat period in the initial aggregate. We propose that the relatively loose packing of the initial aggregate contributes to the indistinctness of the pattern of cross striations and permits internal readjustments toward increased order during fibril formation.

The melting point of the collagen monomer in solution is pH dependent and ranges from 32 to 33° at pH 2.0 to 39–40 at pH 7.0; newly formed fibrils melt at 52° (4, 16, 17). Studies of collagen denaturation at neutral pH, however, are complicated by spontaneous fibril formation and require addition of fibril inhibitors (16, 17). We have examined such solutions and have found abundant numbers of initial aggregates. We conclude that a considerable proportion of collagen in cold physiological solution is not in monomeric form, but is present as aggregates. Furthermore, we suggest that the increase in the inherent stability of the collagen helix with pH is related in part to stability conferred upon collagen by aggregation (4, 18).

The intermolecular forces that effect the formation of the initial aggregates appear to be different from those that involve continued aggregate–aggregate interaction. The several fibril inhibitors used, including Tris, sucrose, and glucose, tend to stabilize water structure and compete for hydrogen bonding sites (11). This would suggest that they inhibit both hydrogen bonding and hydrophobic interactions between collagen aggregates and that the addition of aggregates to each other and to the developing fibril is dependent on hydrophobic interactions, whereas formation of the initial aggregate is more dependent on the charged side chains of the collagen (19).

We consider that the suprafibrillar order, frequently observed in our studies, is of morphogenetic significance, possibly telling us something about the formation of orthogonal collagenous structures in the cornea and skin of many vertebrates (7). Although our understanding of the physical forces involved in such longer range interactions are scanty for biological polymers, these types of supramolecular arrays are commonly found in liquid crystals. That such physical forces are operative on biological polymers seems quite possible, especially in view of the close resemblance of the spiraling orthogonal pattern of collagen in the submammalian cornea (20) to that observed in cholesteric liquid crystal suspensions (21). There is no doubt, however, that these elementary forces are considerably modulated in the biological systems by complicated sequential enzymatic activities, hetero-molecular interactions, and cellular influences (22, 23).

This is Publication no. 699 of the Robert W. Lovett Memorial Group for the Study of Diseases Causing Deformities. This work was supported by Grant AM 3564 from the National Institutes of Health. R. L. T. is a recipient of an American Cancer Society Faculty Research Award (PRA-107).

1. Martin, G. R., Byers, P. H. & Piez, K. A. (1975) *Adv. Enzymol.* **42**, 167–191.
2. Bornstein, P. (1974) *Annu. Rev. Biochem.* **43**, 567–603.
3. Fessler, L. I., Morris, N. P. & Fessler, J. H. (1975) *Proc. Natl. Acad. Sci. USA* **72**, 4905–4909.
4. Gross, J. (1964) *Science* **143**, 960–961.
5. Trelstad, R. L. (1971) *J. Cell Biol.* **48**, 689–694.
6. Weinstock, M. & Leblond, C. P. (1974) *J. Cell Biol.* **60**, 92–127.
7. Trelstad, R. L., Hayashi, K. & Toole, B. P. (1974) *J. Cell Biol.* **62**, 815–830.
8. Trelstad, R. L., Kang, A. H., Toole, B. P. & Gross, J. (1972) *J. Biol. Chem.* **247**, 6469–6473.
9. Bruns, R. R. & Gross, J. (1973) *Biochemistry* **12**, 808–815.
10. Öbrink, B. (1972) *Eur. J. Biochem.* **25**, 563–572.
11. Hayashi, T. & Nagai, Y. (1972) *J. Biochem.* **72**, 749–758.
12. Gross, J. & Kirk, D. (1958) *J. Biol. Chem.* **233**, 355–360.
13. Gross, J. (1956) *J. Biophys. Biochem. Cytol.* 2 (Suppl): 261–274.
14. Wood, G. C. & Keech, M. K. (1960) *Biochem. J.* **75**, 588–598.
15. Miller, A. & Parry, D. A. D. (1973) *J. Mol. Biol.* **75**, 441–447.
16. Dick, Y. P. & Nordwig, A. (1966) *Arch. Biochem. Biophys.* **117**, 466–468.
17. Hayashi, T. & Nagai, Y. (1973) *J. Biochem.* **73**, 999–1006.
18. Flory, P. J. & Garrett, R. R. (1958) *J. Am. Chem. Soc.* **80**, 4836–4845.
19. Hulmes, D. J. S., Miller, A., Parry, D. A. D., Piez, K. A. & Woodhead-Galloway, J. (1973) *J. Mol. Biol.* **79**, 137–148.
20. Trelstad, R. L. & Coulombre, A. J. (1971) *J. Cell Biol.* **50**, 840–858.
21. Bouligand, Y. (1972) *Tissue Cell* **4**, 189–217.
22. Lapiere, C. M. & Nusgens, B. (1974) *Biochim. Biophys. Acta* **342**, 237–246.
23. Trelstad, R. L. (1975) in *Extracellular Matrix Influences on Gene Expression*, eds. Slavkin, H. C. & Greulich, R. C. (Academic Press, New York), pp. 331–339.